

# LYAPUNOV BASED OBSERVER DESIGN FOR FLYBACK CONVERTER

R.KANTHIMATHI<sup>1</sup>, J.KAMALA<sup>2</sup>

Department of Electronics and Communication Engineering,  
College of Engineering Guindy, Anna University, Chennai, India.

[rvkmathi86@yahoo.co.in](mailto:rvkmathi86@yahoo.co.in)<sup>1</sup>, [jkamalaa@annauniv.edu](mailto:jkamalaa@annauniv.edu)<sup>2</sup>

**Abstract:** This paper proposes the design of observer for flyback converter using the Lyapunov direct method. Non-linearity and large signal model are considered for the design. The objective is to design a robust controller to regulate an output voltage of the converter. It will track the reference voltage for wide variation of input voltage and load. Non-linear state feedback control is used to reduce error and improves converter efficiency. Schur's complement method is employed to convert Non-LMI into LMI. It reduces the complexity involved in the mathematical calculations. Observer functionalities are verified through Matlab simulation. It is shown that the Lyapunov observer based control performs better than pole placement controller and PID controller. Error and chaotic behavior of the converter are reduced with Lyapunov controller and compared with other controllers

**Key words:** Flyback converter, State observer, Lyapunov direct method, Non-Linear matrix inequality, chaotic behavior

## 1. Introduction

In DC-DC converters, controlling its output voltage is essential to get the desired value in many applications like power supplies, green energy systems, battery charging and motor control. Generally, flyback converter is more suitable for high voltage and low power (less than 100 W) applications, due to its simplicity, low cost, and galvanic isolation.

Various analog and digital control methods have been used for output voltage regulation. There are three types of control techniques. They are voltage mode control, current mode control and

hysteresis control [1]. In the flyback converter, primary side current control and secondary side voltage control are used [2]. Because of simplicity and zero steady-state error, proportional-integral (PI) controller is used in different dc-dc converters. PI controller tuned using Ziegler Nicholas (ZN) method for the converter is discussed in [3]. Problems associated with stability and current mode PI controller for the converter driving LED load is discussed in [4]. M. M. Abdel Aziz et al [5] described design procedures of different compensation schemes like PI, PID and fuzzy logic control for voltage mode controlled dc-dc switching converters. Flyback converter with digital PI controller is designed for a lithium ion battery charging system and implemented using DSP module [6].

An observer-based digital controller offers additional advantages of hardware saving [7]. It doesn't require additional sensors. Computations are embedded and performed in the controller. Luenberger state observer is designed by one of the following methods. They are pole placement method, Lyapunov based observer and sliding mode observer.

State observer is designed by pole placement technique to achieve the stability of a completely controllable system. The state feedback matrix is optimized using linear quadratic optimal regulator (LQR) method based on Riccati matrix. It improves the system performance [8], [9]. To prove the effectiveness of the observer based digital controller, model predictive control is applied to the flyback converter, which is operating in continuous conduction mode (CCM). Ya Zhang et al [10] designed Luenberger observer using pole placement method.

Because of switching action of the power semiconductor devices, the model is non-linear. Therefore, linear controllers cannot be stable for a wide range of operation. It is not possible to obtain a satisfactory response for a power supply with wide load change using a PI regulator. It is completely well-known that non-linear controllers exhibit more stable and robust response for wide load and input change [11]. In recent years, passivity-based [12], sliding mode [13]-[16], back stepping [17], Lyapunov based [18] and exact feedback linearization controllers [19] are employed in many applications.

The linear matrix inequality (LMI) based method with state estimation using Lyapunov function is explained in [20], [21]. Input variable constraints are considered in the state feedback control of the linear MIMO systems. Lyapunov based control for SEPIC converter is designed with a proof of the asymptotic stability of the observer error using port Hamiltonian formalism is presented in [22]. Hyunki Cho et al. [23] discussed the state observer and controller design of boost converter using the Lyapunov direct method and LMI approach. In this paper design of Lyapunov based prediction observer for flyback converter is proposed and controller design depends on this observer.

Non-linear systems exhibit chaos and bifurcation phenomena. This violates the path of reference tracking system. Control of the chaos with voltage mode and current control have been focused by many researches. Current control chaotic behavior in dc-dc converters is explained in [24], [25]. Lian-Qing [26] proposed control of chaos in buck-boost converter with voltage mode control. In this paper voltage mode chaos control of flyback converter is discussed.

This paper is organized as follows. Section II presents the state model of the flyback converter. In section III Lyapunov based observer and controller design are explained. Simulation results of the converter with observer and controller are given in section IV. Section V is concluded with features of controllers.

## 2. State model of flyback converter

Overall block diagram of converter control is shown in Figure 1. It consists of the flyback converter, observer, and controller. The observer is called as state estimator. It estimates the converter state variables. These values are compared with the reference and produce error signal. Error is reduced according to the controller design and the control signal of the converter is generated to get better performance.

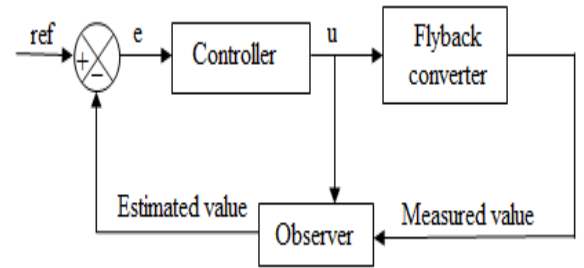


Figure 1: Block diagram

The basic circuit of the converter is shown in Figure 2. It is derived from the buck-boost converter. Based on duty ratio, the output voltage is greater or lesser than the input voltage. The output voltage of converter is given in equation (1).

$$V_o = n V_{in} \left( \frac{u}{(1-u)} \right) \quad (1)$$

$n = \frac{N_2}{N_1}$  - turns ratio of the flyback transformer

$N_1$  - transformer primary number of turns

$N_2$  - transformer secondary number of turns

$V_{in}$  - dc input voltage

$V_o$  - output voltage

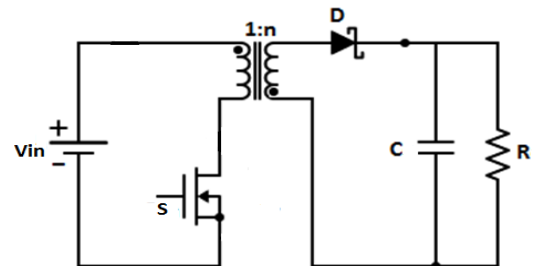


Figure 2: Flyback converter circuit

Its operation is very simple and mainly depends on the transformer's primary current. When

a switch is turned on, the transformer's primary is connected to the supply. The current and magnetic flux in the primary side is increased and energy is stored in it. Since the diode on the secondary side is reverse biased, a negative voltage is induced in it. Output filter capacitor supplies energy to the load. The rising primary current can be written in equation (2).

$$i_L = \frac{V_{in}}{L_m} t_{on} \quad (2)$$

When the switch is turned off, current and magnetic flux in the primary side is decreased. A positive voltage is induced in secondary side, so diode is forward biased. Energy stored in the transformer is delivered to the output capacitor and the load. The decreasing primary current can be written in equation (3).

$$i_L = \frac{-V_o}{nL_m} t_{off} \quad (3)$$

where,  $i_L$  - transformer primary current

$L_m$  - magnetizing inductance of the transformer

$u$  - duty ratio of the switch, which is constrained as  $0 \leq u \leq 1$

$t_{on}$  - turn on period

$t_{off}$  - turn off period

Peak value of primary and secondary current can be calculated as follows,

$$I_{spk} = \frac{2I_o}{1-u} \quad (4a)$$

$$I_{ppk} = I_{spk} \times \frac{N_2}{N_1} \quad (4b)$$

where,  $I_{ppk}$  - primary peak current

$I_{spk}$  - secondary peak current

$I_o$  - output current

Primary and secondary peak current wave forms of the converter are shown in Figure 3. Peak value occurs as the consequence of core loss of transformer and current stress of switching components. In closed loop control peak, the current value is greatly reduced.

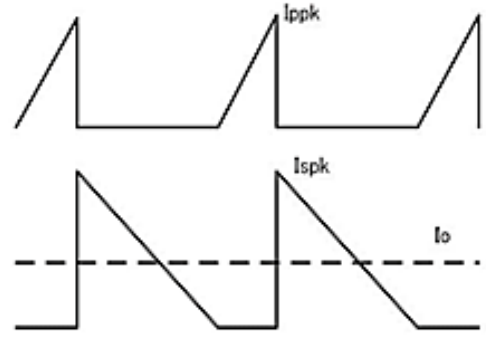


Figure 3: Peak primary and secondary current waveform

The output capacitance used for filter out the ripple content in the output voltage and magnetizing inductance are obtained by the equations

$$C = \frac{V_o \times u}{f_s \times R \times \Delta V_o} \quad (5)$$

$$L_m = \frac{V_{in} \times u}{f_s \times I_{ppk}} \quad (6)$$

where,  $\Delta V_o$  - voltage ripple

$f_s$  - switching frequency

$C$  - output capacitance

$R$  - load resistance

Specifications of the converter for the design are tabulated in Table 1.  $i_L$  and  $V_o$  are considered as two state variables of the flyback converter. The frequency of the switching is taken as 50 kHz.

Table 1: Values of parameters

Parameter	Rating
Input DC voltage, $V_{in}$	50 V
Output DC voltage, $V_o$	100 V
Switching frequency, $f_{sw}$	50 kHz
Transformer turns ratio, $N_p : N_s$	1:2
Magnetizing Inductance, $L_m$	480μH
Output capacitance, $C_o$	220μF
Output resistance, $R_o$	500Ω
Input Power, $P_{in}$	100W

The dynamic equations based on turn on and turn off operations are obtained for one switching period as

$$\dot{i}_L = \frac{V_{in}}{L_m} - (1-u) \frac{V_o}{nL_m} \quad (7a)$$

$$\dot{V}_o = -\frac{V_o}{RC} + (1-u) \frac{i_L}{nC} \quad (7b)$$

The dynamic values of  $i_L$  and  $V_o$  can be controlled by the continuous duty ratio  $u$ , which is obtained from the observer based controller. State model of the converter depends on modes of operation [27], [28]. Large signal model is considered and the operating point can swing throughout the range, it could be nonlinear. Average state space model of the converter as,

$$\begin{aligned} \dot{x} &= Ax + Bu \\ y &= Hx \end{aligned} \quad (8)$$

where,  $x = [i_L \ V_o]^T$  - state vector

$y = V_o$  - system output

A - system matrix

B - input matrix

H - output matrix

$$A = \begin{bmatrix} 0 & \frac{-(1-u)}{nL_m} \\ \frac{(1-u)}{nC} & \frac{(2u-1)}{RC} \end{bmatrix}$$

$$B = \begin{bmatrix} \frac{V_{in}}{L_m} \\ 0 \end{bmatrix} \quad H = \begin{bmatrix} 0 & 1 \end{bmatrix}$$

For 50% duty cycle system matrix and input matrix in continuous domain can be calculated as

$$A = \begin{bmatrix} 0 & -520.83 \\ 1136.36 & 0 \end{bmatrix} \quad B = \begin{bmatrix} 10416667 \\ 0 \end{bmatrix}$$

A discrete-time system is a transformation that maps a given input sequence  $u_k$  into an output sequence  $y_k$ . State and output equations of the discrete-time system are

$$\begin{aligned} x_{k+1} &= Fx_k + Gu_k \\ y_k &= Hx_k \end{aligned} \quad (9)$$

where, F and G depend on the sampling time T, and it can be obtained as following

$$F = e^{AT} \quad \text{and} \quad G = \int_0^T (e^{A\theta} B) d\theta$$

System matrix and input matrix in discrete domain for the sampling period of 20μs can be found as,

$$F = \begin{bmatrix} 0.9998 & -0.0104 \\ 0.0227 & 0.9999 \end{bmatrix} \quad G = \begin{bmatrix} 2.0837 \\ 0.0024 \end{bmatrix}$$

### 3. Lyapunov based observer and controller design

In order to speed up the estimation process, the difference between the measured and the estimated output is given as a feedback and correct the model continuously with this error signal. The main aim of the controller design is to build a suitable robust controller for a nonlinear system that guarantees stability and satisfactory performance of the closed loop system. Lyapunov based direct method is employed to provide robust observer and controller. Figure 4 shows the estimation scheme using discrete time observer.

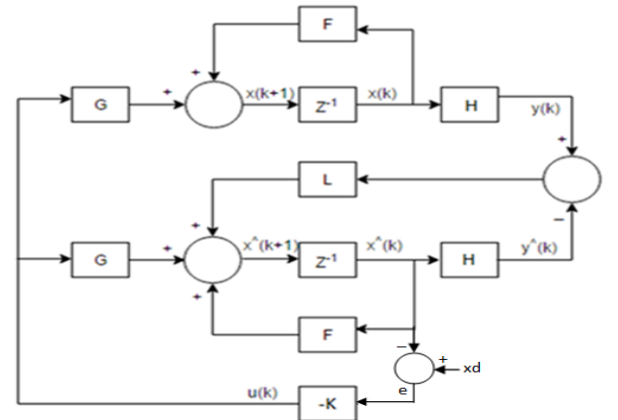


Figure 4: Discrete observer realization

#### 3.1 Luenberger observer

The Luenberger observer is a deterministic type of observer. It is designed to estimate or observe output voltage and primary current of the flyback converter. In this work observer design based on Lyapunov direct method is proposed. The observer is represented as,

$$\hat{x}_{k+1} = F\hat{x}_k + Gu_k + L[y_k - \hat{y}_k] \quad (10)$$

$$\hat{y}_k = H\hat{x}_k$$

where,  $\hat{x}_{k+1}$  - predicted state vector

$\hat{x}_k$  - estimated state vector

$\hat{y}_k$  - estimated output

L - observer gain matrix

$$\hat{x} = [\hat{i}_L \quad \hat{V}_o]^T$$

Estimation error can be represented as  $\tilde{x} = x - \hat{x}$ .

Then the observer error dynamics are defined by

$$\tilde{x}_{k+1} = x_{k+1} - \hat{x}_{k+1} = (F - LH)\tilde{x}_k \quad (11)$$

$\tilde{x} = [\tilde{i}_L \quad \tilde{V}_o]^T$ . Observer implementation in the discrete domain is called as prediction observer. It estimates the states in one sampling period ahead of the measurement  $y_k$ . The Luenberger observer for this discrete-time system is therefore asymptotically stable when the matrix (F-LH) has all the Eigen values inside the unit circle.

### 3.2 Controller Design

The state feedback controller design is based on the observer estimated value. Controller design should be such that, the output voltage must track the reference voltage in steady state. The control law is represented as

$$u_k = -Ke = -K[x_d - \hat{x}_k] \quad (12)$$

where, K - controller gain matrix. Controller error  $e = x_d - \hat{x}$ , then the controller error dynamic of the entire system is represented as

$$e_{k+1} = x_d - \hat{x}_{k+1} = (F - K)e \quad (13)$$

### 3.3 Lyapunov based observer design

Lyapunov direct method is the most important tool for design and analysis of nonlinear systems. It

is directly applied to nonlinear systems without the need to linearization and thus achieves global stability. The basic concept behind this direct method is that if the total energy of a system is continuously dissipating, then the system will eventually reach an equilibrium point and remain at that point. Hence, Lyapunov direct method includes two steps,

1. Find an appropriate scalar function, referred to as a Lyapunov function,
2. Evaluate its first-order time derivative along the trajectory of the system.

Positive definite Lyapunov function consists of both observer and controller error dynamics can be written as

$$V = \tilde{x}^T P \tilde{x} + e^T e \quad (14)$$

The time derivative of lyapunov function can be expressed as

$$V_{k+1} = \tilde{x}^T P \tilde{x}_{k+1} + \tilde{x}_{k+1}^T P \tilde{x} + e_{k+1}^T e_{k+1} + e_{k+1}^T e \quad (15)$$

$V_{k+1}$  should be less negative definite for asymptotic stability. Using equations (11) and (13) it can be written as

$$V_{k+1} = \tilde{x}^T [P(F - LH) + (F - LH)^T P] \tilde{x} + 2e^T (F - K)e < 0 \quad (16)$$

The term in square bracket can be written as,

$$P(F - LH) + (F - LH)^T P < -Q \quad (17)$$

$$PF - LHP + F^T P - L^T H^T P + Q < 0$$

$$PF - F^T P - ZH - Z^T H^T + Q < 0 \quad \text{and} \quad P > 0 \quad (18)$$

P and Q are 2×2 positive definite matrixes. Take, Z=PL. Equation (18) is the nonlinear matrix inequality (Non-LMI) equation. Convert Non-LMI to LMI using Schur complement.

$$\begin{bmatrix} PF - F^T P - ZH - Z^T H^T + Q & 0 \\ 0 & -P \end{bmatrix} < 0 \quad (19)$$

$$P = \begin{bmatrix} 2.5 & 0 \\ 0 & 2.5 \end{bmatrix} \quad Q = -\begin{bmatrix} 7.48 & 0.015 \\ 0.015 & 1.5 \end{bmatrix}$$

$$Z = \begin{bmatrix} 0.015 \\ 3 \end{bmatrix} \quad F = \begin{bmatrix} 0.634 \\ 1.199 \end{bmatrix} \quad K = [0.126 \quad 0.268]$$

The behavior of the Luenberger observer based controller is simulated in Matlab Simulink with operating frequency of 50 kHz. Simulation is done with the different controller such as pole placement controller, Lyapunov observer based controller and PID controller and their results are compared.



The diagram illustrates a control system for a motor. It starts with a reference voltage  $V_{ref}$  (100) and a feedback voltage  $V_o^A$  (1). These are combined at a summing junction to produce an error signal  $e$ . This error signal is then multiplied by a gain  $K \cdot u$  (gain1) to produce a control signal  $u$  (1). This control signal is then multiplied by another gain  $K \cdot u$  (gain) to produce a signal that is compared with a reference value (0000 00) at a relational operator ( $\geq$ ). The output of the relational operator is a data type conversion block (double), which is then delayed by 2 units to produce a signal  $d$  (2). This signal  $d$  is then used to generate a gate pulse (Gate pulse) for the motor. The entire system is labeled Generator1.

Figure 6 shows the controller implementation. It generates the control signal to get regulated output voltage. The gate pulse generation of closed loop simulation is shown in Figure 7. Gate pulse is derived by comparing carrier and error signal. On period of the gate pulse is  $10\mu\text{s}$  for 50 kHz switching frequency.

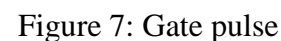


Figure 10 is a line graph titled "Primary and Secondary current". The x-axis is labeled "Time (s)" and ranges from 0 to 0.1 with major ticks every 0.01 seconds. The y-axis is labeled "Current (A)" and ranges from 0 to 1.2 with major ticks every 0.2 Amperes. There are two data series: "Primary current" represented by a solid red line and "Secondary current" represented by a dashed blue line. The primary current shows a series of sharp, periodic peaks that decrease in amplitude over time, starting at approximately 1.1 A and ending around 0.7 A. The secondary current shows a series of broader, periodic peaks that also decrease in amplitude over time, starting at approximately 0.6 A and ending around 0.4 A. The peaks of the secondary current occur slightly after the peaks of the primary current.

This is the effective and easiest method to find the observer gain. The system tracks the reference



accurately. The observer and controller gain for Lyapunov and pole placement methods are given in Table 2.

Table 2: Observer and controller gain

Method	Observer gain	Controller gain
Lyapunov	$[0.634 \ 1.199]^T$	$[0.126 \ 0.268]$
Pole placement	$[3.61 \ 8.3]^T$	$[0.174 \ 0.307]$

The estimated primary current and output voltage waveforms are shown in Figure 9 and Figure 10 respectively and the average values are tabulated in Table 3.

Table 3: Estimated values of current and voltage

Variables	Measured value	Estimated value
Primary current	0.7A	0.1A
Output voltage	99.8V	99.2V

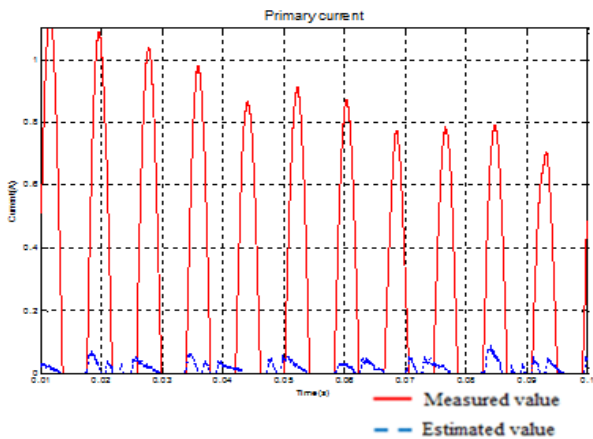


Figure 9: Primary current waveform

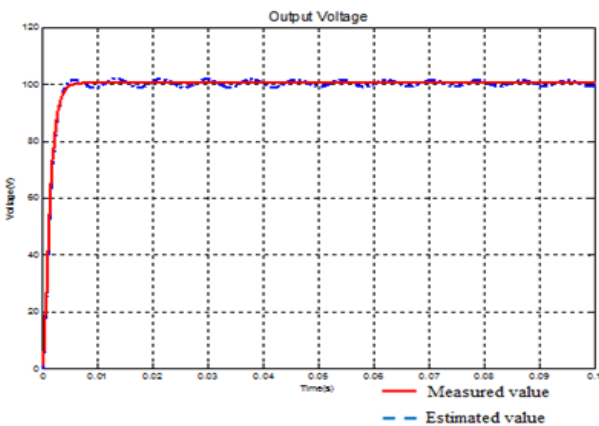


Figure 10: Output voltage waveform

The output voltage and output current are settled at 0.34 ms and a fast dynamic response is obtained. It is given in Figure 11.

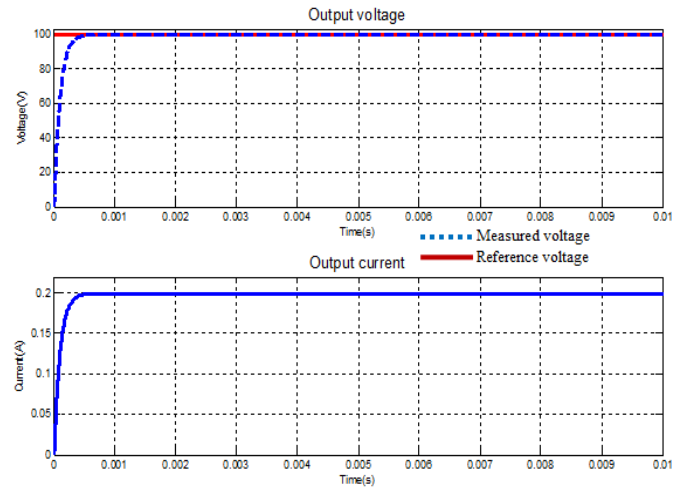


Figure 11: Output voltage and current waveforms

Table 4: Output voltage and %Error

Load Resistance ( $\Omega$ )	Lyapunav observer based controller		Pole placement controller		PID controller	
	$V_o$ (V)	Error (%)	$V_o$ (V)	Error (%)	$V_o$ (V)	Error (%)
50	98.9	1.14	89.4	10.6	94.8	5.2
100	99.3	0.7	93.9	6.1	97	3
200	99.5	0.47	96.7	3.3	98.2	1.78
300	99.6	0.4	97.3	2.67	98.6	1.44
400	99.7	0.36	97.8	2.22	98.7	1.25
500	99.8	0.2	98.3	1.74	98.9	1.13

$i_L$  and  $V_o$  are estimated without using any sensors. The output voltage exactly tracks the reference. No overshoot occurs. For various load resistance values, the readings are taken with different controllers and tabulated in Table 4.

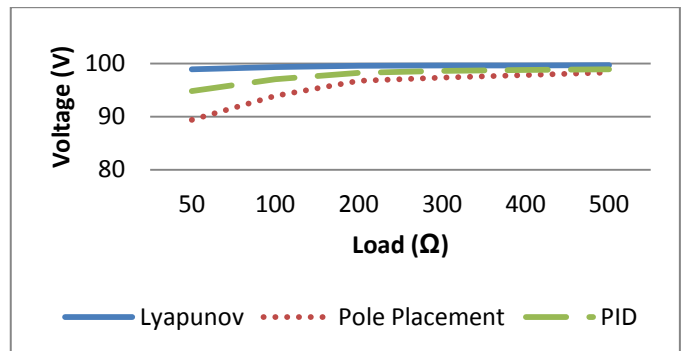


Figure 12: Output voltages for load variation

Output voltage response for wide variation of the load resistance is shown in Figure 12. It is noted that at light load condition (5-100 $\Omega$ ), the Lyapunov controller tracks the reference approximately with the error of (1.14%). For the wide variation of load (200-500 $\Omega$ ), it exactly follows the reference with 0.34% of error. From this, it is confirmed that robust controller can be designed using Lyapunov stability method.

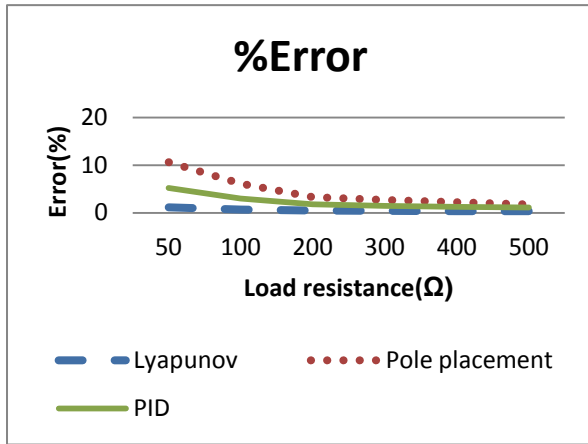


Figure 13: Load resistance versus % error

Percentage of error for various load resistance is given in Figure 13. If  $R_o$  is increased, the error is reduced. With Lyapunov based observer controller, reduction of error can be achieved.

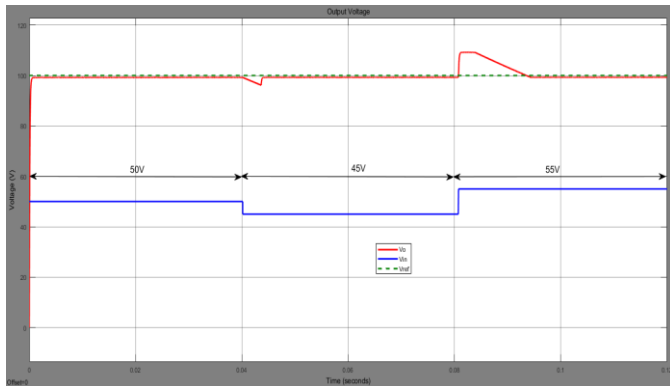


Figure 14: Output voltages for input supply variation

For input supply variation ranges from 45-55V the output voltage track the reference efficiently with this robust controller and it is shown in Figure 14. Only settling time can be varied.  $V_o$  is settled at 5ms for (50 to 45V) changes

and 19ms for (45 to 55V). Lyapunov observer based controller is compared with pole placement controller and PID controller for a 500 $\Omega$  resistive load. The readings are tabulated in Table 5. From the output voltage waveform shown in Figure 15, it is proved that Lyapunov observer based controller offers better results.

Table 5: Results with different controllers

Type of controller	I <sub>in</sub> (A)	I <sub>o</sub> (A)	V <sub>o</sub> (V)	t <sub>r</sub> (ms)	t <sub>s</sub> (ms)	Error (%)
Lyapunov	0.7	0.199	99.8	0.33	0.8	0.2
Pole placement	1.71	0.196	98.3	2.3	7	1.74
PID	1.74	0.198	98.9	1.1	3	1.13

The total power losses of the flyback converter for three types of controller are tabulated in Table 6. Losses include transformer losses, semiconductor device losses, diode and capacitance losses. Lyapunov controller speed up the response and quick reference tracking is achieved. This reduces switching losses and gate driving losses of the converter. Based on input and output current variation remaining losses are varied for each controller. Losses of the converter with different controllers for varying load are shown in Figure 15.

Table 6: Losses of the converter with different controllers

Load Resistance ( $\Omega$ )	Lyapunov observer based controller	Pole placement controller	PID controller
	P <sub>losses</sub> (W)	P <sub>losses</sub> (W)	P <sub>losses</sub> (W)
50	10.13	15.84	12.97
100	9.4	13.4	11.3
200	8.01	12.8	9.65
300	7.88	11.6	8.73
400	7.84	10.32	8.16
500	7.8	9.45	7.89

Timing parameters and percentage error of different controllers are compared and given in Figure 16. It can be observed that Lyapunov



observer based controller and PID controller are giving the good performance.

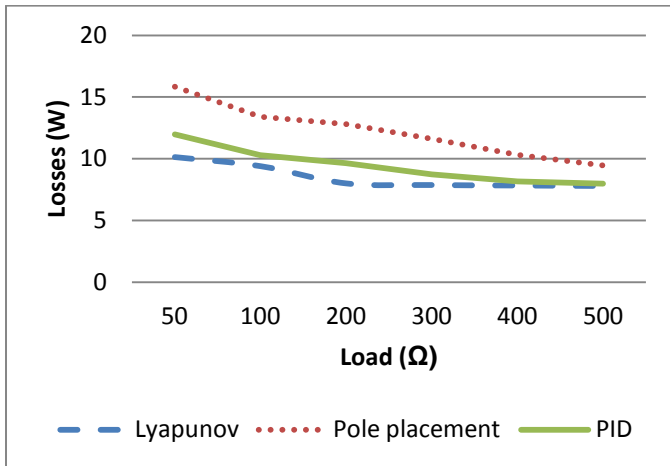


Figure 15: Comparison of controllers

Rise time ( $t_r$ ), fall time ( $t_s$ ), and %error of these type of controllers are less when compared with pole placement controller. The reason is that poles are located on the unit circle in root locus plot. It will slow down the system dynamics and settling time is reduced. With PID controller by arbitrary choosing of gain values, some extent these problems can be rectified.

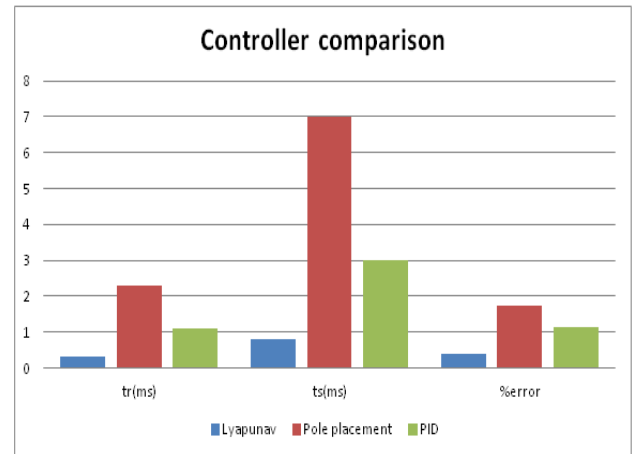


Figure 17: Comparison of controllers

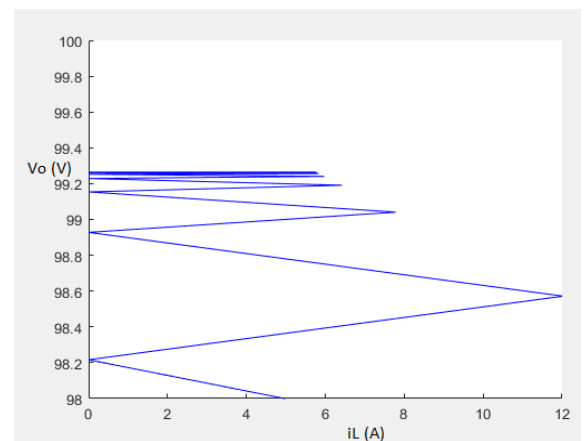


Figure 18: Phase portrait of chaotic behavior

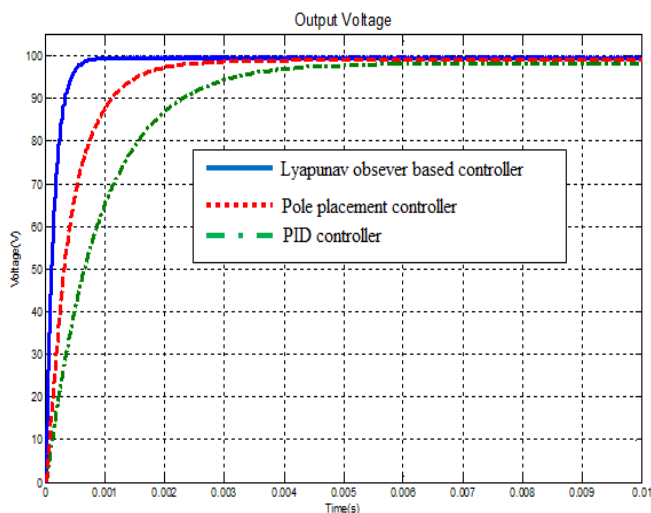


Figure 16: Comparison waveform of output voltage

Lyapunov observer based controller performs better and estimates the states of the system without using the sensor, compared with PID controller.  $t_r$ ,  $t_s$ , and percentage error values are 0.33ms, 0.8ms, and 0.4% respectively. These values are very less. It is the great advantage of this controller and suitable for most dc-dc converter control.

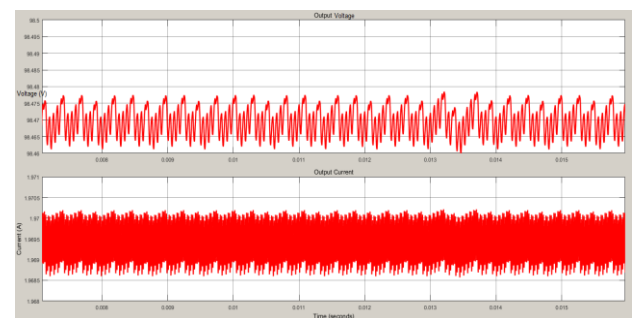


Figure 19: Chaotic behavior of  $V_o$  and  $i_L$

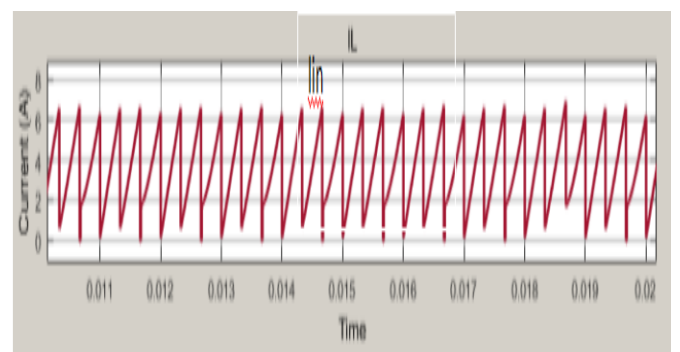


Figure 20: Primary current with chaotic control

The phase plot of chaotic operation is shown in Figure 18. Chaos behavior of the state variables is shown in Figure 19. With voltage mode control, Lyapunov observer based controller eliminates the chaotic behavior. Figure 20 and Figure 21 show chaotic controlled primary current and output voltage respectively.

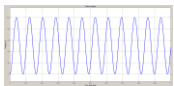


Figure 21: Output voltage with chaotic control

## Conclusion

Lyapunov observer based controller is designed for the flyback converter. Primary current and output voltage can be estimated using observer without sensors. Controller reduces the error and the output voltage exactly tracks the reference value.  $t_r$ ,  $t_s$ , and percentage error values are very less when compared with other controllers. The computation requires five addition, seven multiplication and two delay blocks. It reduces complexity.

Since the output is settled in less time (0.8ms), simulation time is very less (1s). The fast dynamic response is achieved. Stable and reliable nonlinear system can be obtained with the help of Lyapunov observer. It is proven with software implementation. Power losses are reduced with this controller. Also it eliminates chaotic behavior with voltage mode control.

## References

- [1] Prajal S Chavan, M.F.A.R.Satarkar.: *Overview of control technique for dc-dc converters*, IRF Int. Conf., 2015, p. 51-55.
- [2] Tsung-Yao Chiang et al.: *An observer design for primary side control of flyback converter*, IEEE Int. Conf. on System Science and Engineering, 2010, p. 358-363.
- [3] Abhinav Dogra and Kanchan Pal.: *Designing and tuning of PI controller for flyback converter*, Int. Journal of Engineering Trends and Technology, Vol. 13, No. 3, 2014, p. 117-122.
- [4] Pong M. H. Bryan.: *A stability issue with current mode control flyback converter driving LEDs*, IEEE-IPEMC, 2009, p. 1402-1406.
- [5] M. M. Abdel Aziz et al.: *Simplified approaches for controlling dc-dc power converters*, Int. Journal of Engineering Science and Technology, Vol. 4, No. 2, 2012, p. 792- 804.
- [6] Paul C.P. Chao et al.: *A battery charge controller realized by a flyback converter with digital primary side regulation for mobile phones*, Springer-Verlag Berlin Heidelberg, Microsystems technology, 2014, p. 1689–1703.
- [7] Djekidel Kamri and Cherif Larbes.: *Observer based control for dc–dc converters practical switching control*, Arabian Journal for Science and Engineering-Springer, 2014, p. 4089–4102.
- [8] R.Shenbagalakshmi and T.Sree Renga Raja.: *Observer based pole placement and linear quadratic optimization for dc-dc converters*, Journal of Electrical Engineering, p. 1-8.
- [9] Mohammed Alkrunz and Irfan Yazici.: *Design of discrete time controllers for the DC-DC boost converter*, Sakarya University Journal of the Institute of Science and Technology, Vol.20, No.1, 2016, p. 75-82.
- [10] Ya Zhang et al.: *CCM flyback converter using an observer-based digital controller*, IEEE Int. Conf. on Industrial Technology, 2015, p. 2056-2061.
- [11] Gionata Cimini et al.: *Robust current observer design for dc-dc converters*, Int. Conf. on Renewable Energy Research and Applications, 2014, p. 19-22.
- [12] N. Gonzalez-Fonseca et al.: *Observer based controller for switch-mode dc-dc converters*, IEEE Conf. on Decision and Control, 2005, p. 4773-4778.
- [13] K. Ramesh Kumar, S. Jeevananthan, and S. Ramamurthy.: *Improved performance of the positive output elementary split inductor-type*

*boost converter using sliding mode controller plus fuzzy logic controller*, WSEAS TRANSACTIONS on systems and control Vol. 9, 2014, p. 215-228.

- [14] Xutao Li, Minjie Chen and Tsutomu Yoshihara,: *Design of sliding mode observer based sensor-less control of boost converter for high dynamic performance*, Journal of signal processing, Vol. 19, No. 6, 2015, p. 253-261.
- [15] Mahdi Salimi,: *Sliding mode control of the dc-dc flyback converter with zero steady-state error*, Journal of basic and applied scientific research, Vol. 2, 2012, p.10693-10705.
- [16] A. Bennassar, M. Barara, A. Abbou and M. Akherraz,: *Performance evaluation of sliding mode control for induction motor based on the fuzzy Luenberger observer and Kalman filter*, Journal of Electrical Engineering, p. 1-8.
- [17] Adel Zakipour and MahdiSalimi,: *On back-stepping controller design in buck/boost dc-dc converter*, Int. Conf. on electrical, electronics and civil engineering, 2011, p. 147-151.
- [18] Stefan Köhler et al.,: *Lyapunov based nonlinear observer design for an inductively supplied saturated excitation coil of an externally excited synchronous machine*, 2015, p. 1-8.
- [19] Mahdi Salimi and Samira Siami,: *Close loop control of dc-dc buck converters based on exact feedback linearization*”, IEEE Conf. 2015.
- [20] Anna Filasov.A and Dusan Krokavec,: *State estimate based control design using the unified algebraic approach*, Archives of Control Sciences, Vol. 20, No. 1, 2010, p. 5–1.
- [21] Chi-Tsong Chen,: *Linear system theory and design*, Oxford University Press, 1999.
- [22] A.R. Meghnous, M. T. Pham and X. Lin-Shi,: *Nonlinear observer and Lyapunov-based control for SEPIC converter: Design and experimental results*, American Control Conf., 2013, p. 5833-5838.
- [23] Hyunki Cho, Sung Jin Yoo and Sangshin Kwak,: *State observer based sensor less control using Lyapunov method for boost converters*, IET Power Electronics, Vol. 8, No. 1, 2015, p. 11–19.
- [24] Kiran, N,: *Control of chaos in positive output LUO converter by means of time delay feedback*, International Electrical Engineering Journal (IEEJ), 2015, Vol. 6, No. 2, p. 1787-1791.
- [25] Fu, C. B., Tian, A. H., Yu, K. N., Lin, Y. H., & Yau, H. T. : *Analysis and control of chaotic behavior in dc-dc converters*, Mathematical Problems in Engineering, 2018.
- [26] Lian-Qing, Z., & Yi, P,: *Chaos control of voltage mode controlled buck-boost converter*, Acta Physica Sinica, 2016, Vol. 65, No. 22.
- [27] Sanjeev Kumar Pandey, S.L.Patil, and Vijaya S. Rajguru,: *Isolated flyback converter designing, modeling and suitable control strategies*, Int. Conf. on Advances in Power Electronics and Instrumentation Engineering, 2014, p. 47-58.
- [28] R.Shenbagalakshmi and T.Sree Renga Raja,: *An observer-based controller for current mode control of an interleaved boost converter*, Turkish Journal of electrical engineering & computer sciences, Vol. 22, 2014, p. 341-352.